International RILEM Conference on Materials, Systems and Structures in Civil Engineering
Conference segment on Service Life of Cement-Based Materials and Structures
22-24 August 2016, Technical University of Denmark, Lyngby, Denmark

HARDENING INDUCED STRESSES IN VERY THICK CONCRETE MEMBERS – INSIGHTS FROM COMPREHENSIVE FE-STUDIES

Peter Joachim Heinrich [(1)], Dirk Schlicke [(1)]

(1) Graz University of Technology, Graz, Austria

Abstract
This contribution presents first results of comprehensive FE-studies on hardening-induced stress histories of very thick concrete members with compact dimensions. The motivation is to improve the understanding of their structural behaviour in order to provide an efficient but safe crack width control of such members. The strict application of current design rules would lead to very high reinforcement amounts, even though observations in practice indicate that serviceability can be ensured with much less reinforcement. Finally, the insights of these investigations will provide a basis on which efficient design rules can be developed for very thick concrete members. The FE-studies were conducted with a new constitutive law for hardening concrete whereby special regard was put on the influence of the member thickness, the ambient temperature as well as production conditions. In general, the results confirm the predominance of residual stresses or so called Eigenstresses in such structural elements, while restraint forces and restraint moments are of minor importance for usual subsoil conditions.

1. Introduction

Very thick concrete members experience remarkable temperature histories due to hardening since the majority of the heat, which is released during the exothermal cement hydration, is firstly stored in the interior of the member before it flows out very slow according to the limited thermal conductivity of the concrete. These temperature histories are characterized by transient temperature field changes consisting of uniformly (constant) in the cross section distributed parts, temperature gradients over the cross sections width and height as well as non-linear parts resulting from temperature differences between the interior and the surface regions of the member. The accompanying temperature deformations lead to thermal stresses according to the restraining situation. In general, very thick members usually have rather compact dimensions. Former investigations show that such members are predominantly stressed by the non-linear parts, which are almost completely restrained since the cross

section tends to remain plane. At the same time, real length changes due to constant parts and curvatures due to temperature gradients are hardly restrained. The main reason is the very high axial stiffness of the hardening member itself and the limited bending restraint of members with low length-to-height ratios.

Although the precise dimensions of hardening-induced residual stresses and their interaction with additional restraints due to seasonal temperature changes are needed for an efficient structural design of very thick and compact concrete members, this has not been investigated systematically yet. Neither national nor international design rules provide satisfying design rules of such special cases because they are rather based on empiricism than on mechanically consistent aspects, see [1]. Thus, the main aim of the presented studies is to develop a mechanically consistent design concept that takes geometric dimensions, boundary conditions and/or the material properties itself into account with special regard to the safety-concept of Eurocode 2 [2].

2. Calculation model

A reliable determination of the resulting stress distribution calls for a comprehensive time-step calculation model, which uses well-established material models as well as realistic boundary conditions. Here, a FE-based model is generated in the modular FE-framework SOFiSTiK. Its mesh is exemplified for the reference case of the study in Fig. 1. It can be seen that the mesh is refined in the surface regions because of the expected higher influence of the ambient temperature.

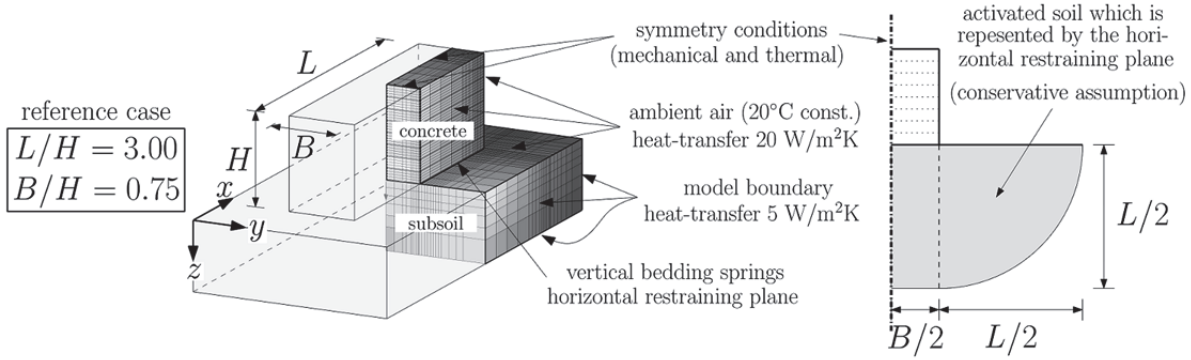

Figure 1: FE-Mesh

To generate a regular mesh, the included module SOFIMSHA uses given geometric node definitions. For each time-step, the module HYDRA determines the temperature-field in the structure. Later, the module ASE follows the procedure and calculates the resulting stresses, while it takes the temperature-field directly from HYDRA as thermal loading. The module SOFILOAD applies additional loads, e.g. further deformation impact from shrinking.

At this point, it should be mentioned that the calculation model was comprehensively verified by satisfying recalculations of in-situ monitorings of several mass concrete applications, e.g. a 4.0 m thick power plant slab or a 2.5 m thick chamber wall of a sluice. Further details are given in [3].

2.1 Structural idealization

The basic model consists of several 3D elements (8 nodes with linear shape functions) and it represents only a quarter of the whole structure. This reduces the complexity of the calculation and increases the speed of the whole simulation. Appropriate boundary conditions consider the symmetry as well as bedding and thermal conditions. During the temperature-field calculation, the modelled soil acts as heat storage. For the stress calculation, the soil body is replaced by a vertical bedding with non-linear compression-springs and horizontally arranged 2D elements (4 nodes with linear shape functions). The vertical bedding springs allow a realistic self-weight activation in cases of temperature gradients over the height as well as eccentric external restraint at the bottom of the member. This is of major importance in the considered cases with length-to-height ratios of three. The horizontal soil stiffness will be represented by the horizontally arranged 2D elements with regard to the activated soil below the member, as illustrated in Fig. 1.

The structures dimensions are fully variable in every direction; it is possible to control each surrounding condition and furthermore to investigate different types of construction-methods (e.g. fresh-in-fresh concrete placement in layers).

2.2 Simulated material behaviour and models used

The simulated material behaviour represents a typical mass concrete with a strength class of C35/45. All relevant properties of this concrete are extensively presented, cf. [3]. The hardening process of this concrete was simulated time-discretely with a thermo-mechanical coupling on basis of the so-called equivalent (effective) concrete age. The equivalent concrete age is a state variable that takes the maturity (influence of the real concrete temperature in the structure on the speed of hydration and hardening) into account. In the applied material model, this state variable controls the release of hydration heat by the JONASSON approach, the simultaneously developing strength properties of the hardening concrete by the WESCHE approach, the appearance of autogenous shrinkage as well as the viscoelastic behaviour according to the stress history by an approach proposed by SCHLICKE. In particular, the occurring viscoelastic strains of a time step were determined according to a time-discrete analysis of the EC2 creep curves and implemented independently for each element and direction in every time step. Further details are given in [3] and [4].

2.3. Analysis of the determined temperature and stress fields

The results of such an analysis are temperature and stress fields for each time step. On the one hand, it is important to know their absolute values in the material points (nodal results) to assess the risk of cracking. On the other hand, it is important to draw clear conclusions on the restraining situation as well as the type of cracking. Thus, it is important to analyse these fields with regard to uniformly (constant), gradual (linear) and non-linear distributed parts that can directly be related to stress resultants and residual stresses or so-called Eigenstresses. In general, it can be said that

- the *constant* temperature-part leads to an expansion or shortening of the member in the considered direction and this results in case of external restraint in a force or in case with eccentric restraining in a force and two bending moments (an inner moment according to the cross section compatibility and an outer moment according to self-weight activation)

- the *linear* temperature-part leads to a curvature of the cross section around the considered axis and this results in the case of restraint in another bending moment and
- the *non-linear* temperature-part is self-balanced within the cross section and has therefore no resultants. However, these deformations are usually almost fully restrained by the plane cross section, which leads to residual stresses, or so-called "Eigenstresses" which are also self-balanced within the cross section.

The following part gives a short summary of the separation of an arbitrary resulting temperature- or stress-field into the described parts. The procedure is in general the same for both of them. At this point it should be noted that the stress field changes are solely caused by the relative temperature field changes. For a comparison of both, the analysis of the temperature field changes has therefore to be done separately in each time step only for the change in this time step. The course of the specific part can then be drawn by summing up the single changes per time step. There exist a few ways to perform the temperature- or stress-field separation: [4] and [5] describe one simple and efficient way, if resulting temperature- or stress-fields are more or less "well" known in advance. If the resulting distributions are more "doubtful", it is better to use the way of a general (numerical) integration of the temperature- or stress-field over the whole cross-section. This is possible, if the temperature- or stress-field is known as a function $f(y, z)$. Here, a MATLAB-routine is used to determine these functions for each single time-step by the usage of a 2D-least-squares-fit for a fourth-order-polynomial in y and z. Fig. 2 illustrates the procedure of fitting, integration and separation respectively.

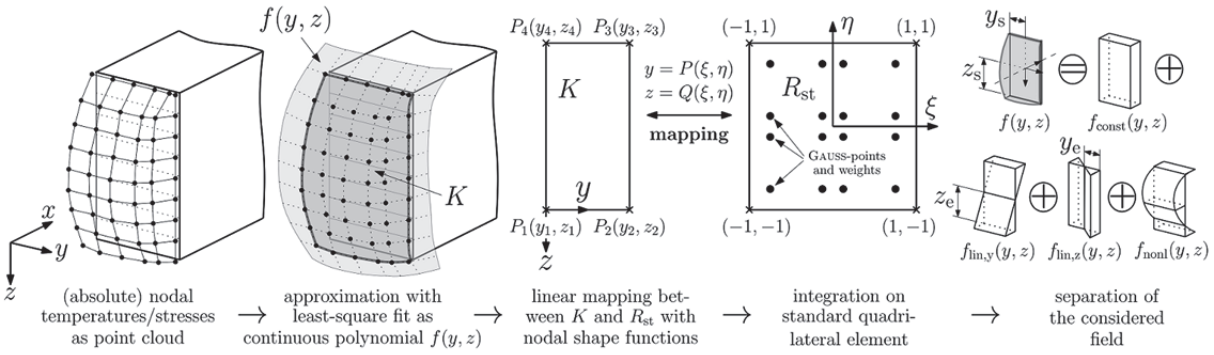

Figure 2: fitting, integration and separation of an arbitrary temperature- or stress-field

After the fitting, it is possible to integrate the received functions over the region K. A numerical well-established way is to use a 2D-GAUSSian quadrature formula of order N, given in (1). The mapping $x = P(\xi, \eta)$ and $y = Q(\xi, \eta)$ can be achieved conveniently by using nodal shape functions; $J(\xi, \eta)$ is the Jacobian of the transformation, and w_i, w_j are the weights, see [6].

$$\int\int_K f(y,z)\,\mathrm{d}y\mathrm{d}z \approx \sum_{i=1}^{N}\sum_{j=1}^{N} w_i \cdot w_j \cdot f\left(P(\xi_i,\xi_j), Q(\xi_i,\xi_j)\right) \cdot \left|J(\xi_i,\xi_j)\right| \tag{1}$$

Dividing (1) by the area of the considered cross-section leads to the resulting constant part, (2). Multiplying each point of (1) by its moment arm in z-direction and dividing it finally by the corresponding moment of inertia around the y-axis multiplied by the distance z_e from the

centre of gravity, leads to the corresponding linear part around y. The linear part around z could be gained analogous (3).

$$f_{\text{const}} = \frac{1}{A_{\text{c}}} \cdot \left(\sum_{i=1}^{N} \sum_{j=1}^{N} w_i \cdot w_j \cdot f\left(P(\xi_i, \xi_j), Q(\xi_i, \xi_j)\right) \cdot \left|J(\xi_i, \xi_j)\right| \right) \tag{2}$$

$$f_{\text{lin,y,e}} = \frac{1}{I_{\text{y}} \cdot z_{\text{e}}} \left(\sum_{i=1}^{N} \sum_{j=1}^{N} w_i \cdot w_j \cdot f\left(P(\xi_i, \xi_j), Q(\xi_i, \xi_j)\right) \cdot \left|J(\xi_i, \xi_j)\right| \cdot (z_{i,j} - z_{\text{s}}) \right) \tag{3}$$

Subtracting $f_{\text{const.}}(y, z)$, $f_{\text{lin.,y}}(y, z)$ and $f_{\text{lin.,z}}(y, z)$ from the original distribution $f(y, z)$ finally leads to the residual part $f_{\text{nonl.}}(y, z)$. Note that if the geometry and the boundary as well as the loading conditions are symmetric to one axis, the corresponding linear part is zero. For the present case, this is the case for the zx-plane so that $f_{\text{lin,z}}(y,z)$ is not pursued any further.

3. Case Study

3.1 Set up and investigated parameters

From a geometric point of view all considered cases represent a kind of "bloc", neither a slab (because $B \sim H$) nor a wall (because $H / B << 4$). Besides, all cases have an L / H-ratio of 3 which is the lower boundary to be considered as a wall – even if this is a common ratio to define the length of a construction stage respectively the distance between expansion joints of walls. The case study investigates the variation of several factors that are known to influence the temperature- and stress-field in ground slabs as well as in walls on foundations significantly. The variation of these factors varies within the range of typical conditions of practical cases. It is possible to summarize these conditions in three groups, which are geometry, initial and ambient temperatures and material/construction. Here, the presented results solely display the reference concrete C35/45. Fig. 3 shows the set up of the study and the different cases that have been simulated.

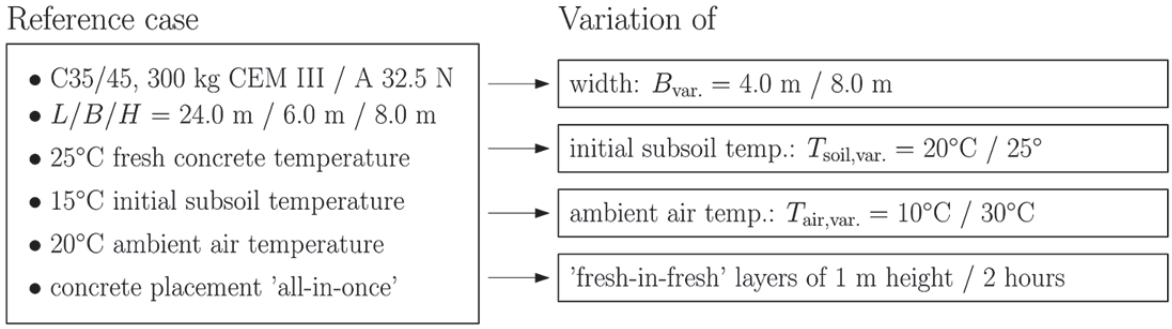

Figure 3: parameter variation of the case study

Any other boundary condition is similar in all cases. This refers mainly to the heat exchange over the free surfaces which is set with 20 W/m²K without any further consideration of formwork and its removal. The heat exchange at the bottom depends on the thermal properties

of the soil, whereby a conductivity of 1.6 W/Km and a thermal capacity of 1900 kJ/Km³ has been considered. The support in the bedding area was estimated according to the stiffness of common subsoil. In vertical direction, a stiffness of 10 000 kN/m³ was considered in case of compression whereas the transfer of vertical tensile forces in the bedding was totally excluded with the non-linear bedding springs. In contrast to this very realistic assumption in vertical direction, the horizontal restraint in the bedding area was set up to a value, up to where macrocracking cannot be excluded for the reference case, as explained in section 3.2.

3.2 Results of the reference case

Fig. 4 gives the course of absolute results in selected nodes in the symmetry in length direction. It can be seen that the structure reaches its absolute temperature maximum at t = 160 h (~60°C), while temperature equalization occurs after about 5 months. As expected, there are huge temperature differences within the cross section with almost adiabatic conditions in the interior, whereas the temperatures on the free surfaces are very close to the ambient air temperature and do not pass 30°C. The temperatures at the bottom increase delayed but are still remarkable. The accompanying stresses reflect this temperature impacts only partly: on the one hand, the resulting stresses of a given temperature change in a time step increase during the hardening according to the stiffness evolution; on the other hand, viscoelastic effects distort the course considerably. But what one can see already is the predominance of Eigenstresses since almost all absolute stresses of the surface have an opposite sign as the interior stresses. Besides, the comparison of absolute stresses in Fig. 4 with the mean value of the lower limit of the tensile strength ($f_{ctk;0.05}$) indicates that cracking cannot be excluded in general.

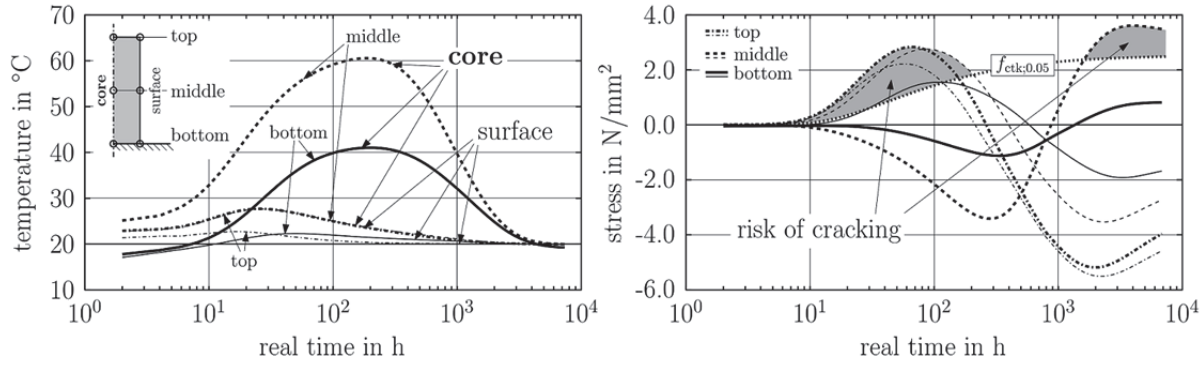

Figure 4: nodal results (temperature and stress) of the reference case

To clarify the type of cracking to be expected, Fig. 5 gives the course of constant and linear parts in the temperature and stress field history. Linear parts around the *z*-axis were not pursued since they are zero in the considered case due to symmetrical conditions over the width as remarked in section 2.3. As mentioned before, the horizontal restraining condition in the bedding area was iteratively increased up to where macrocracking would occur in the reference case. Hereby, the risk of macrocracking is assessed by the comparison between maximum stresses due to restraint force and restraint moments ($\sigma_{const.+lin.,y,bottom}$) with the mean value of the tensile strength (f_{ctm}). Eigenstresses, however, are neglected since they are self-balanced in the cross section and have therefore no significant influence on macrocracking. Further details on this assumption are given in [7] and [8].

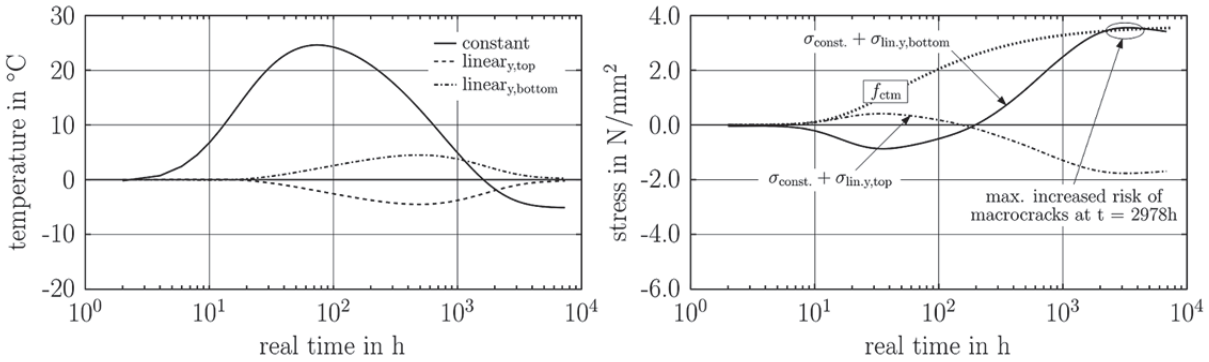

Figure 5: analysis of temperature and stress field changes of the reference case

As expected, macrocracking would predominantly result from the constant temperature changes, which are huge in these thick members. However, the eccentric restraining of these parts at the member bottom in combination with a limited *L* / *H*-ratio causes always a distinct linearity in the stress distribution over the height. Altogether, the risk of macrocracks is the highest at temperature equalization where restraint force and restraint moment superimpose both in tension at the bottom. The indicated risk of macrocracks is very low in this example since the required horizontal subsoil stiffness exceeds conventional conditions by several orders of magnitude (over 10 000 times higher in this case). Of course, this factor would vary since subsoil activation depends predominantly on the member length, however, increasing *L* / *H* would also reduce critical linearity in the stress distribution over the height and thus require higher horizontal stiffness.
In case of a realistic consideration of horizontal subsoil stiffness, restraint force and restraint moments are much smaller, whereas Eigenstresses would remain in the above shown size. Thus, the risk of macrocracks is usually very small, whereas the risk of microcracks as well as locally restricted cracks is still very high at early ages in the surface region. At temperature equalization, the risk of microcracks is also indicated in the interior, but this is overestimated since all calculations assume a fully linear-elastic cross section which is not the case for the surface region after early cracking.

3.3 Parameter variation

Fig. 6 and Fig. 7 show the determined courses of temperatures and stresses in the specific points at the surface and in the interior for all considered cases.

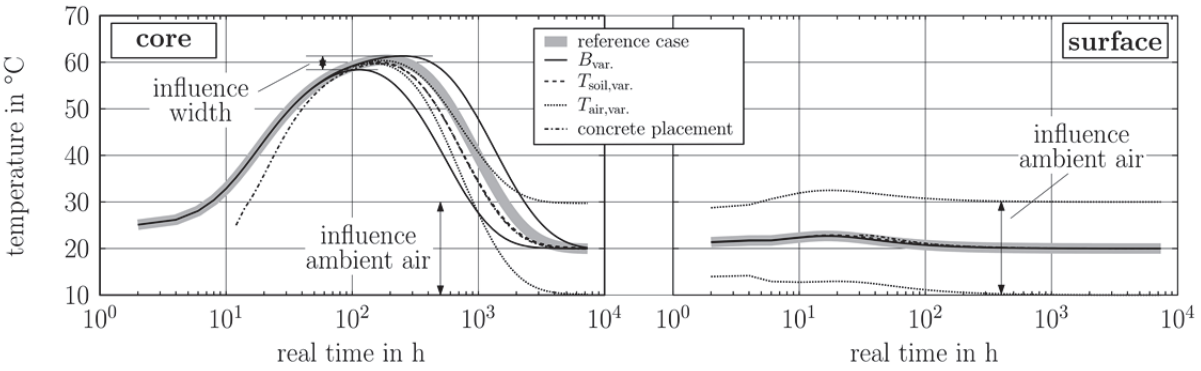

Figure 6: absolute temperatures in specific core- and surface-points

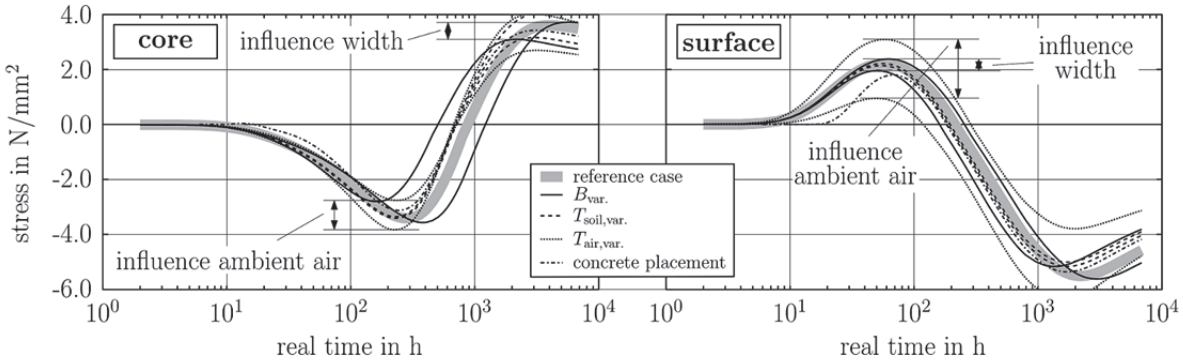

Figure 7: total stress in specific core-and surface-points

Fig. 8 and Fig. 9 show the course of the constant and linear temperature parts around the *y*-axis, whereby the stress resultants are illustrated in form of a superposition at the members bottom to see the most critical value in tension.

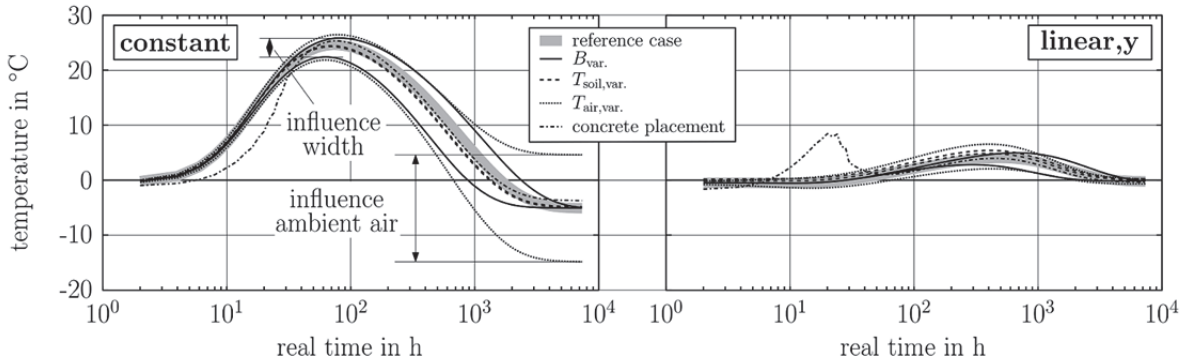

Figure 8: constant and linear (bottom) temperature part

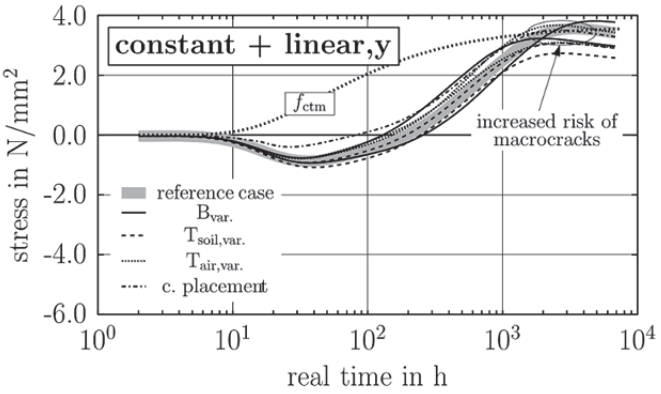

Figure 9: superposition of constant and linear (bottom) stress part

4. Discussion

4.1 General findings

As expected, very thick concrete members show a significant hardening-induced temperature history consisting of huge constant temperature changes as well as significant temperature

differences within the cross section. The accompanying stress field consists predominantly of Eigenstresses whereas the build up of critical restraint forces and restraint moments would require very high external restraint which is in the present case around 10 000 times higher than the horizontal stiffness of conventional soil.

4.2 Influence of member width

Although the member width has a clear influence on the duration of the whole process, the effect on absolute resulting stresses is small. The main reason is that there are almost adiabatic conditions in each member anyway so that the differences in the deformation impacts are insignificant.

4.3 Influence of subsoil temperature

The subsoil temperature has a significant influence on the temperature history at the bottom of the thick member. This affects the temperature gradients. Depending on the bending restraint this could increase the risk of bending cracks at temperature equalization in case of much stiffer subsoil. In the considered conditions this is of minor importance. Here, solely the effect on the absolute maximum temperature in the interior matters in terms of intensification of surface cracking.

4.4 Influence of ambient air temperature

Of course, the ambient air temperature has a significant influence on the temperature field. But as in the previous cases, the effect on the risk of macrocracking is rather small due to the limited external restraint. What can be said is that a delayed decrease of ambient air temperature after casting will have a negative effect on the intensity of surface cracking.

4.5 Influence of construction method

If the process of concrete placement is taken into account, the temperature and stress field are significantly influenced in the beginning. However, decisive stresses are comparable with the results without consideration of the process of concrete placement. Of course, this statement is only valid for temperature induced stresses. In reality, the construction process introduces high tensile stresses at the bottom due to the higher stiffness in the bottom layer when the new layer will be placed. However, the latter affects also the viscoelastic behaviour which depends on the absolute stresses.

5. Conclusion and Outlook

Considering the resulting temperature-parts, only the variation of width as well as the variation of the ambient temperature have a significant influence on the constant part. Linear parts were not influenced significantly in any case. Finally, it has to be outlined that none of the parameters has a high influence neither on the restraint force nor on the restraint moments. This leads to the conclusion that typical compact mass concrete members are predominantly stressed by Eigenstresses. The expected crack pattern of such members will be characterized by surface cracking, whereby these cracks may reach a depth up to 1.0 m.

It should be noted that all cases show huge constant temperature changes. A critical restraining of these deformations is very unlikely since it requires very high external restraint which is in the present case around 10 000 times higher than the horizontal stiffness of conventional soil. Of course, this factor would vary since subsoil activation depends

predominantly on the member length, however, the factor would also not decrease significantly for longer members since its size depends on the linearity in the stress distribution according to L / H as well. And even if a macrocrack could be triggered at the bottom, separating cracks over the whole member height can still be excluded for L / H ratios smaller or equal to three. The reason is that the stress distribution without Eigenstresses has in such cases still a distinct linearity due to the eccentric localization of the restraining condition at the bottom. Hereby, the top of the member is always significantly compressed when the tensile strength may be reached at the bottom, which gives cracks stopping by itself in the lower part of the member.
There have to be done further investigations, concerning the continuance of the present parametric study which should be expanded on more influence factors. Such factors are the investigation of various thermal boundary conditions (like retaining walls, or underwater structures), various geometrical conditions (mainly increasing L / H) or various bedding conditions.

Another essential step will be the superposition with further deformation impacts due to seasonal changes of ambient temperature.

Acknowledgement

This research project is funded by Austrian Research Promotion Agency (FFG), pr.-nr. 843489.

References

[1] Heinrich, J. P. and Schlicke, D.: Normative Regelungen zur unbewehrten Ausführung von massigen Betonbauteilen, In: Proceedings of 2. Grazer Betonkolloquium, Graz, (2014)
[2] EN 1992-1-1:2004 + AC:2008: Eurocode 2: Design of concrete structures - Part 1-1: General rules and rules for buildings
[3] Schlicke, D.: Mindestbewehrung für zwangbeanspruchten Beton, PhD thesis, Graz University of Technology (2014) http://lamp.tugraz.at/~karl/verlagspdf/buch_schlicke_25052016.pdf
[4] Schlicke, D.: Consideration of Viscoelasticity in Time Step FEM-Based Restraint Analyses of Hardening Concrete, Journal of Modern Physics 4 (2013), SCIRP, 9-14
[5] Eierle, B. and Schikora, K.: Zwang und Rissbildung infolge Hydrataionswärme – Grundlagen, Berechnungsmodelle und Tragverhalten, DAfStb Heft 512, Berlin (2000)
[6] Shaozhong, D.: Quadrature Formulas in Two Dimensions, online Lecture notes http://math2.uncc.edu/~shaodeng/TEACHING/math5172/Lectures/Lect_15.PDF (date of access: 11.04.2016), University of North Carolina at Charlotte (2010)
[7] Schlicke, D. and Tue, N. V.: Crack width control – verification of the deformation compatibility vs. covering the cracking force, Proceedings of MSSCE2016/Service Life Segment, Lyngby, Denmark (2016)
[8] Knoppik-Wróbel, A. and Schlicke, D.: Computational prediction of restraint-induced crack patterns in reinforced concrete walls. In: Proceedings of MSSCE2016 / Service Life Segment, Lyngby, Denmark (2016)